Analyst

ROYAL SOCIETY OF CHEMISTRY

PAPER

View Article Online
View Journal | View Issue

Check for updates

Cite this: *Analyst*, 2025, **150**, 1151

An amplification-free digital droplet assay for influenza A viral RNA based on CRISPR/Cas13a†

Jiayan Liu,[a,b] Taixue An,[c] Jingjie Peng,[b] Qinjiang Zhu,[d] Heyang Zhao,[b] Zhiyu Liang,[a] Kai Mo, *[d] Tiancai Liu *[b] and Kun Wu*[a]

Received 12th October 2024,
Accepted 29th January 2025

DOI: 10.1039/d4an01328j

rsc.li/analyst

Most of the CRISPR-based RNA detection methods are combined with amplification to improve sensitivity, which lead to some drawbacks such as aerosol pollution, complicated operation, and amplification bias. To address the above issues, we developed a digital detection method for influenza A viral RNA based on droplet microfluidics and CRISPR/Cas13a without polymerase chain reaction. We used a microsphere coupled to a capture probe to extract and concentrate the target RNA from the samples, and then restricted the target-induced CRISPR/Cas13a cleavage event to microfluidic droplets, thus enhancing the local signal intensity and enabling single-molecule detection. With a detection limit of 10 copies per μL, influenza A viral RNA can be detected in less than 1 h. Both clinical and synthetic series samples were used to validate the assay's performance. With the help of this direct RNA diagnostic method, a variety of RNA molecules can be easily and accurately detected at the single-molecule level. This research has broad prospects in clinical applications.

Published on 14 febbraio 2025. Downloaded on 14/02/2026 03:50:15.

Introduction

There are four types of influenza viruses (IV): A, B, C, and D.[1] Among them, influenza A viruses (IVA) are among the most dangerous to people, particularly to children and the elderly.[2] It can cause extremely contagious respiratory infections in a variety of creatures, including people, pigs, horses, bats, poultry, and wild migratory birds.[3] More than a century has gone since the 1918 Spanish flu pandemic, which was brought on by IVA.[4,5] There are now 18 hemagglutinin (HA) and 11 neuraminidase (NA) subtypes of IVA known to exist.[6] IVA are thought to have high potential for spreading over the world and causing a large number of diseases and severe economic damage. They also pose a persistent threat to public health security.[7]

Currently, polymerase chain reaction (PCR)-based assays are the most reliable tools for the clinical diagnosis of IVA in respiratory specimens.[8–10] However, PCR-based tests are expensive, require specially trained technicians and advanced laboratory equipment, and take several hours to provide diagnostic results. As a result, the application of PCR-based methods for rapid point-of-care (POC) diagnostics is limited.[11] To circumvent the problems associated with PCR, researchers have employed isothermal nucleic acid amplification techniques, such as loop-mediated isothermal amplification (LAMP), which do not require a thermal cycler to diagnose IV. However, the specificity of these diagnostic assays may also be problematic.[12] There is a need for a fast and accurate diagnostic platform that will allow us to contain influenza outbreaks at an early stage and better control future outbreaks.[13]

The CRISPR/Cas13a system is a CRISPR/Cas class 2 system that recognizes and cleaves the target sequence (also known as cis-cleavage), leading to inadvertent nucleic acid cleavage activity or trans-cleavage.[12] Viral nucleic acids can be precisely and sensitively identified *in vitro* thanks to this collateral action. Microfluidics is seen as a miniaturized "lab-on-a-chip" that allows time-consuming and labour-intensive operations to be integrated into miniature devices.[14–16] When compared to conventional in-tube reactions, the reaction volume is reduced in microfluidics, increasing the concentration of the target/template and speeding up the analytical process.[17]

[a]*Department of Pathogen Biology, Guangdong Provincial Key Laboratory of Tropical Disease Research, School of Public Health, Southern Medical University, Guangzhou, 510515, China. E-mail: wksmu@163.com*
[b]*Key Laboratory of Antibody Engineering of Guangdong Higher Education Institutes, School of Laboratory Medicine and Biotechnology, Southern Medical University, Guangzhou 510515, China. E-mail: liutc@smu.edu.cn*
[c]*Department of Laboratory Medicine, Nanfang Hospital, Southern Medical University, Guangzhou 510515, China*
[d]*Department of Anesthesiology, Zhujiang Hospital, Southern Medical University, Middle Gongye Avenue No. 253, Guangzhou, China. E-mail: mokai303@163.com*
† Electronic supplementary information (ESI) available. See DOI: https://doi.org/10.1039/d4an01328j

Published on 14 febbraio 2025. Downloaded on 14/02/2026 03:50:15.

In order to merge amplification, reactions, and detection onto a small platform, microfluidics combined with CRISPR/Cas systems for virus detection have been created. This lowers the risk of contamination while simultaneously improving the sensitivity and simplicity of detection. There have been reports of several platforms for droplet microfluidics with CRISPR/Cas13a RNA detection recently. For example, highly sensitive and specific nucleic acid detection can be accomplished by combining Cas13a collateral effects with recombinant polymerase amplification (RPA) alone.[18–22] Nevertheless, nucleic acid amplification-based (NAA) techniques invariably result in a number of disadvantages that hinder precise nucleic acid measurement, including the need for costly reagents, several processes, and a higher likelihood of false positives during the amplification process. Because of this, a number of platforms that do not require amplification have also been developed. Bruch, Richard *et al.* presented the first microfluidic integrated electrochemical biosensor for the *in situ* detection of microRNAs that is driven by CRISPR/Cas13a. It is possible to achieve a detection limit of 10 pM.[23] An automated POC system for Ebola RNA detection was reported by Qin, Peiwu, and colleagues.[24] Tian, Tian *et al.* avoided the need for NAA and reverse transcription (RT) by developing an ultra-localized Cas13a assay for single-molecule RNA diagnostics.[25] A POC microfluidic device that permits ultra-sensitive and quick detection of viral RNA in clinical samples without the requirement for sample pre-amplification was also described by Zhang, Yuxuan, and colleagues.[26] Using droplet microfluidics and CRISPR/Cas13a, Shan, Xiaoyun *et al.* created a highly specific and sensitive digital detection approach for SARS-CoV-2 RNA that does not require NAA. SARS-CoV-2 RNA has a detection limit of 470 aM, making it easy to find within 30 minutes.[27] This amplification-free digital detection technique, which is based on CRISPR/Cas13a and droplet microfluidics, offers a promising way for RNA detection in clinical diagnostics and establishes the groundwork for a crucial piece of technology for practical POC diagnostic platforms. However, more data are still required to validate these technologies.

Motivated by this, we utilized polystyrene microspheres to capture and separate the target RNA. We then used a negative pressure-driven droplet microfluidic chip to create droplets and formed a droplet array in the collection chamber to perform subsequent fluorescence imaging after half an hour of the reaction at 37 °C. The target molecule was digitally detected without the need for NAA in less than 1 h, with a 10 copies per μL detection limit. Clinical samples and artificial IVA M gene fragment RNA were used to validate the assay.

Materials and methods

Reagents and materials

LwaCas13a protein was obtained from GenScript Biotech Co., Ltd (China, CAS no.: Z03486). 1-(3-Dimethylaminopropyl)-3-ethylcarbodiimide hydrochloride (EDC-HCL) was obtained from Yeasen Biotechnology (Shanghai) Co., Ltd (China, CAS no.: 60380ES25). *N*-Hydroxysuccinimide (NHS) was obtained from Sigma-Aldrich (Shanghai, China, CAS no.: 6066-82-6). A 384-well plate was obtained from Corning (catalog no.: 3575). DEPC-treated water (DNase-/RNase-free) and streptavidin were purchased from Beijing Solarbio Science & Technology Co., Ltd (CAS no.: Z03486 and S9171). Mineral oil was obtained from Shanghai Acmec Biochemical Technology Co., Ltd (CAS no.: Z03486 and S9171). Droplet generation oil for the probes was obtained from Bio-Rad Laboratories (Shanghai) Co., Ltd (CAS no.: 1863005). The 2× UTaq PCR MasterMix kit (low ROX) was obtained from Beijing Zoman Biotechnolgy Co., Ltd. Opti-Link™ carboxyl-modified polystyrene microspheres were obtained from Thermo Fisher Scientific (Shanghai, China, CAS no.: W500CA). The HiScribe™ T7 quick high yield RNA synthesis kit was obtained from Nanjing Vazyme Biotech Co., Ltd (China, CAS no.: TR101-02). Lysis buffer was obtained from Chenxue-Biotech. All oligonucleotides used in this work were synthesized by Guangzhou IGE Biotechnology Ltd and their sequences are listed in Table S1.†

Preparation of crRNA and the target RNA by *in vitro* transcription

A multi-sequence alignment of all the M gene fragment sequences of influenza A virus available on NCBI was first performed (DNAMAN 9, Lynnon Biosoft, CA, USA). The most conserved region, spanning several hundred base pairs, was selected as a template for amplification and *in vitro* transcription to obtain RNA (ESI Table 2†). Then, Primer Premier 5 software was used to design PCR primers, and the T7 RNA polymerase promoter sequence was appended to the 5′ end of the upstream primer (ESI Table 1†). The target RNA template underwent PCR amplification and gel purification. Subsequently, it was transcribed into RNA *in vitro* using the T7 transcription kit. The resultant purified target RNA was measured using Thermo Fisher Scientific's Nanodrop 2000, diluted, and aliquoted before being kept at −80 °C until needed. The transcribed RNA was then used as a standard for subsequent experiments. T7 RNA polymerase-mediated transcription reaction was carried out to produce crRNA. The reaction mixture consisted of 1× reaction buffer, NTP solution, a specific quantity of the denaturing annealed product (DNA template), and the T7 RNA polymerase mixture. The total volume was 20 μL. The reaction process lasted 16 hours at 37 °C. Thermo Fisher Scientific's Nanodrop 2000 was used to measure the concentration of the purified transcript, which was subsequently stored at −80 °C until needed.

In-tube CRISPR/Cas13a assay

A specific quantity of the target RNA, 100 nM LbuCas13a, 100 nM crRNA, and 150 nM FQ5U RNA reporter were used, and 1× reaction buffer was used to make up the volume of the Cas13a reaction mixture to 20 μL. The list of RNA series is shown in ESI Table 1† which includes the target RNA, crRNA, and the RNA reporter sequence. A 1420 multilabel counter victor3 V device was used to detect fluorescence. The process was carried on for 40 minutes at 37 °C, and fluorescence was collected every 10 minutes.

 This journal is © The Royal Society of Chemistry 2025

Published on 14 febbraio 2025. Downloaded on 14/02/2026 03:50:15.

Design of microfluidic chips

The microfluidic chips were designed based on the channel architecture and dimensions of the standard BioRad ddPCR chip, with the addition of an array chamber at the terminus of the droplet generation section. This array chamber is specifically intended to collect droplets, facilitating the formation of a droplet array that is optimized for subsequent imaging.

Generation and imagination of monodisperse droplets

Prior to droplet generation, the microfluidic chip was filled with an oil phase (droplet generation oil for probes (BIO-RAD)). Then, a disposable plastic syringe was connected to the outlet of the chip through a length of Teflon tubing, 20 μL of the Cas13a reaction mixture were added to the dispersed phase inlet, and 70 μL of droplet generation oil for probes (BIO-RAD) were added into the oil phase inlet. The piston of the syringe was pulled outward and a binder was used to lock in a volume of one milliliter to generate droplets. After the collection chamber was filled with the droplets, the piston was gently pushed back to its starting position. After reacting at 37 °C for 30 minutes, the droplet array was then photographed under a microscope combined into a panoramic scan (EVOS® FL Auto). After the image was obtained, an algorithm for image edge enhancement was applied to improve the brightness of the edge regions.

Optimization of the droplet CRISPR/Cas13a assay conditions

The Cas13a reaction mixture was mixed with varying amounts of the target RNA, and fluorescence was measured every ten minutes for 40 minutes at 37 °C in the 1420 multilabel counter victor3 V device. The reaction termination time for the subsequent droplet Cas13a detection was determined to be the reaction time corresponding to the peak fluorescence value. To figure out the reaction concentration of the RNA reporter in the droplet Cas13a mixture, the concentration of the RNA fluorescent probe was adjusted and all the fluorescent probes in the droplets were enzymatically digested. The concentration of the RNA reporter that emitted bright green fluorescence was applied in the next stage.

Enrichment of the target RNA by polystyrene microspheres

The carboxylate polystyrene microspheres were activated by EDC/NHS and incubated with streptavidin to covalently bind streptavidin. An 18 bp biotinylated DNA capture probe was created based on the target RNA series. Subsequently, the streptavidin-attached microspheres were incubated with biotinylated DNA capture probes for 1 h at room temperature to conjugate the microspheres to the DNA capture probes. Then we captured the RNA with polystyrene microspheres for 20 min.

Digital detection for the target RNA

All RNA molecules were captured during the incubation of the same number of polystyrene microspheres with varying concentrations of the target RNA. Since the number of droplets is much larger than the number of microspheres, at most one microsphere was captured on each droplet. Because of the droplet limiting effect, the concentration of the target RNA was amplified and this will restrict the amount of fluorescence produced by the non-specific transcribed RNA fluorescent probe of Cas13a to the droplet after reacting at 37 °C for 30 minutes. So, the droplets that contain the target RNA were enough to be lit up and recognized by the naked eye. For a single test, ImageJ was used to count the number of droplets within a certain size range in the bright-field image, whereas the corresponding fluorescence images were used to discriminate the positive droplets with a signal-to-noise ratio above 2. The proportion of the positive droplets indicates the concentration of the input sample, in accordance with the Poisson distribution principle.

Clinical evaluation

Patient samples were obtained from Nanfang Hospital, Southern Medical University. All experiments were performed in accordance with the guidelines of Southern Medical University and approved by the ethics committee at Southern Medical University. Informed consent was obtained from human participants of this study.

Human nasopharyngeal swab samples were collected and stored in an inactivated virus preservation solution. Lysis buffer was mixed with the clinical throat swab sample and rinsed multiple times to separate the cells, and the RNA was freed after five minutes. Next, polystyrene microspheres conjugated to DNA capture probes (PSs-P) were added to the lysis buffer, and the RNA was captured for twenty minutes before being centrifuged to extract the target RNA. The assay analysis was then carried out using afDDA and RT-qPCR.

Results and discussion

Principle of the amplification-free digital droplet assay based on CRISPR/Cas13a

Streptavidin-coated polystyrene microspheres were conjugated with biotinylated DNA capture probes that are complementary to the target sequence. After incubation with the sample, the microspheres captured the target and the target was isolated by centrifugation (Fig. 1A). The target-trapped polystyrene microsphere suspension formed a dispersed phase with the Cas13a reaction mixture, which was loaded into the inlet of the aqueous phase, and the fluorinated oil entered through the inlet of the oil phase for shearing (Fig. 1). We used a microfluidic chip to disperse the 20 μL mixture into 2×10^4 droplets and form a droplet array (as shown in Fig. 1B).

Following half an hour incubation at 37 °C, the crRNA in the droplet identified the target sequence captured on the microsphere. This recognition triggered the trans-cleavage activity of Cas13a, which in turn cleaved the fluorescent probe within the droplet. When the fluorescence intensity reached a certain threshold, the droplet illuminated and turned into a positive droplet, denoted as "1". When the droplets failed to

Published on 14 febbraio 2025. Downloaded on 14/02/2026 03:50:15.

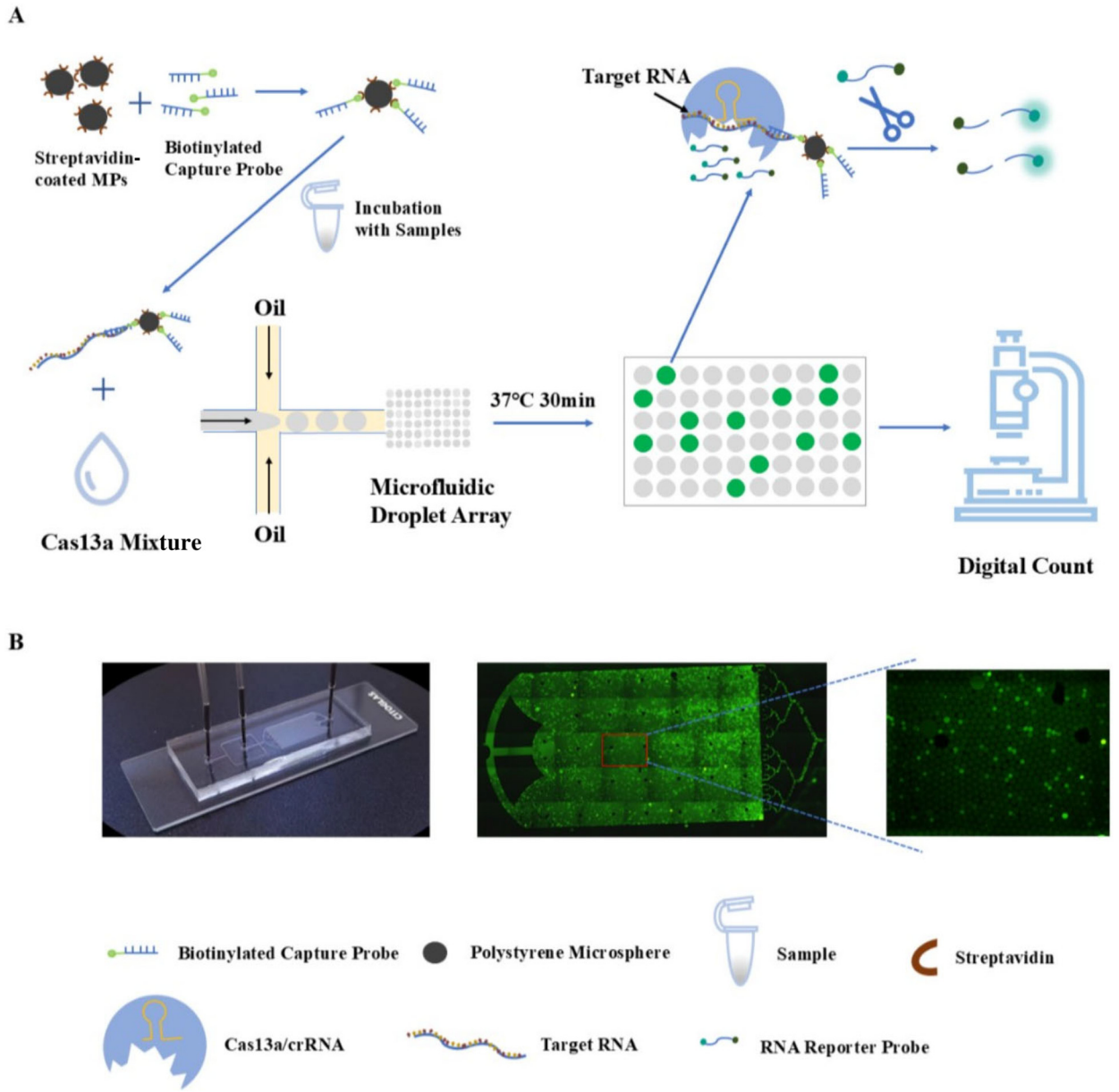

Fig. 1 Scheme of the amplification-free digital droplet assay. (A) Polystyrene microspheres capture targets. Target RNAs together with a Cas13a mixture were emulsified with an oil into thousands of picoliter-sized droplet reactors. After recognition by crRNA (yellow), single-target RNA will trigger the trans-cleavage activity of Cas13a, thus cleaving the fluorescent probe and yielding a fluorescently positive droplet. (B) The microfluidic chip used to generate droplets and the representative scanned fluorescence images of the microdroplet array.

enclose the microsphere or contained one but lacked the target RNA on them, the fluorescent probe cannot be cleaved, the trans-cleavage activity of Cas13a was not triggered, and the droplet cannot light up, and it was a negative droplet, represented as "0" (Fig. 1A). We used the software ImageJ to calculate the fluorescence value of the droplet. We identified the droplet with a fluorescence value higher than the fluorescence value of the negative droplet twice as a positive droplet under the same conditions. When the fluorescence value exceeded this threshold, it can be judged as a positive droplet, and below this threshold, it was judged as a negative droplet. The absolute number of target molecules can be calculated by counting the number of positive and total droplets obeying the Poisson distribution:

$$P(x = k) = \frac{e^{-\lambda}}{k!}\lambda^k \quad (k = 0, 1, 2, 3 \ldots)$$

The variable λ represents the average amount of target molecules in each droplet, whereas k denotes the total number of target molecules in the droplet. $P(x > 0)$ indicates the proportion of positive droplets, which is equal to the ratio of the number of positive droplets to the total number of droplets.

This journal is © The Royal Society of Chemistry 2025

Published on 14 febbraio 2025. Downloaded on 14/02/2026 03:50:15.

$P(x = k)$ indicates the fraction of droplets containing k target molecules. Therefore, the ratio of positive droplets can be used to compute the concentration of λ and the target RNA (c):

$$c = \frac{\lambda}{N_A V}$$

N_A is Avogadro's constant and V is the volume of the droplet.

Generation of monodisperse droplets

We used polystyrene microspheres conjugated to a capture probe to extract the target sequence from the sample. We hybridized a dye-labeled complementary probe to a polystyrene sphere conjugated with a capture probe to validate the microsphere conjugation. As shown in Fig. 2A, an increase in fluorescence was observed in the microspheres conjugated with the capture probe, while no fluorescence enhancement was detected in the uncoupled microspheres, indicating the absence of hybridization to the uncoupled microspheres. This fluorescence was quantified using both flow cytometry and fluorescence microscopy.

It takes a long time to equilibrate and reagents are wasted when monodisperse droplets are formed using positive pressure. Therefore, we used a microfluidic chip to generate droplets under negative pressure, and a 20 μL mixture formed 2×10^5 droplets. Most droplets contained only one microsphere (Fig. 2C). A portion of the droplets was collected and injected into the oil–oil interface formed by mineral oil and fluorinated oil, and the droplets float between the two layers of oil and self-assemble into an array of monodisperse layer droplets. The droplet size obtained in this way is relatively accurate. The droplet array was placed under a microscope to precisely measure the size. As seen in Fig. 2B and C, the droplets generated have an average diameter of 55 μm and were highly homogeneous.

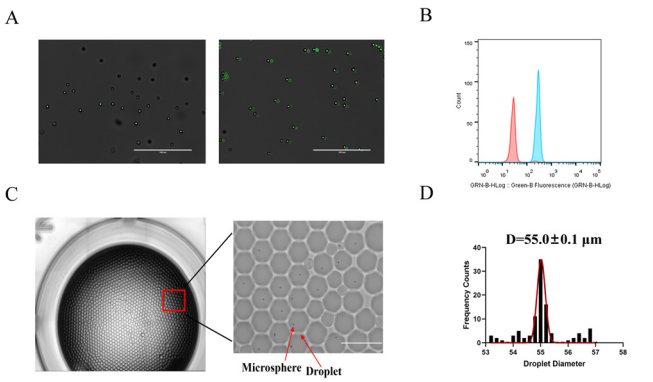

Fig. 2 Generation of monodisperse droplets. (A and B) Coupling validation of microspheres. (A) Fluorescence images of conjugated and unconjugated microspheres after incubation with dye-labeled complementary probes. (B) Flow cytometry validation of conjugated and unconjugated microspheres after incubation with dye-labeled complementary probes. Pink is unconjugated and blue is conjugated. (C) Droplet array at the interface of mineral oil and fluorinated oil (the black dots in the droplets are microspheres) (scale bar is 100 μm). (D) Size distribution of the droplets.

Optimization of the Cas13a reaction system

A sequence on the M gene segment of IVA was chosen as the target sequence10 for detection (Fig. 3A and Fig. S1†), and the specific sequence information is shown in the ESI.† As can be seen in Fig. 3B, only the experimental group with the matching target sequence was able to trigger Cas13a's trans-cleavage activity and cause fluorescence, whereas the groups with the incorrect target of interest and without the sequence were unable to do so.

The Cas13a reaction time was determined to be 30 minutes; for that, various target RNA concentrations were supplied to the reaction system and the fluorescence values of the experimental groups at various concentrations peaked at that time (Fig. 3C). The fluorescent probe's final concentration in the PCR tube was 150 nM. The fluorescence intensity of the microdroplets was not intense enough to be observed by fluorescence microscopy when we employed a concentration of 150 nM despite the fact that all of the probes had been severed. As a result, we increased the fluorescent probes' concentration. A brilliant fluorescence image of the droplet can be obtained (Fig. 3D) as the probe concentration reaches 5 μM. Consequently, the ultimate probe concentration for the ensuing reactions was set at 5 μM.

Single-molecule IVA RNA detection and quantification

We chose a serial dilution of IVA RNA (10–10^5 copies per μL) and added them to the Cas13a reaction mixture in a total volume of 20 μL to validate the effectiveness of droplet microfluidics-based digital detection of CRISPR/Cas13a. To determine the fraction of positive droplets, the total number of droplets and the number of positive droplets in each series of chips were computed. A positive droplet is identified by a fluorescence value with a signal-to-noise ratio above 2. It was evident that the number of positive droplets increases as the

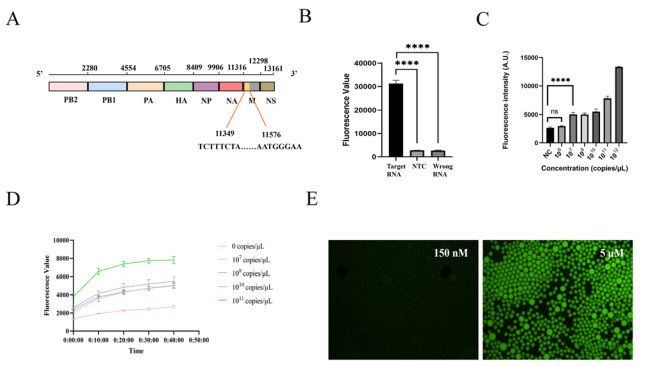

Fig. 3 Optimization of the digital droplet Cas13a reaction system. (A) Target sequences for IVA detection. (B) Validation of the specificity of crRNA. (C) Detection limit of the Cas13a reaction in the tube. (D) Time course of Cas13a detection at different target concentrations incubated at 37 °C. (E) Fluorescence images of two concentrations of the fluorescent probe in the digital droplet Cas13a assay.

Published on 14 febbraio 2025. Downloaded on 14/02/2026 03:50:15.

concentration increases (10–10^7 copies per μL), and at the target concentration of 10 copies per μL, the number of positive droplets was equal to that of the negative control group. The partial fluorescence imaging of droplets from various chip concentration series is displayed in Fig. 4A, where it is evident that the input concentration and the proportion of positive droplets are clearly correlated. The results are shown from three replicates, and in the dynamic range of concentrations of 10–10^5 copies per μL, a strong linear response (R^2 = 0.9914) was also seen between the measured and input concentrations (Fig. 4B). Alternatively, the droplet digital Cas13a test demonstrated a sensitivity increase of almost 10^6 times that of the in-tube Cas13a assay, with the latter only able to achieve a detection limit of 10^7 copies per μL (Fig. 3C).

Clinical evaluation

In the clinical sample testing experiment, we selected 9 clinical nasopharyngeal swab samples to evaluate the clinical performance of our method. These swabs were collected from patients who have been clinically diagnosed with influenza A. The linear quantitation range for the IVA RNA using RT-qPCR was from 10^2 to 10^{12} copies per μL (S4). In line with the RT-qPCR findings, our approach yielded 100% detection of 9 positive samples, with RT-qPCR detecting a ninth sample at extremely low amounts (Fig. 5C). Fig. 5A shows a representative green fluorescence image of sample 8. Simultaneously, our approach produced a false positive error out of 10 negative samples (Fig. 5B), while RT-qPCR successfully identified 10 negative samples. The outcomes demonstrated that the afDDA approach performed well and might satisfy the criteria for influenza A clinical sample detection.

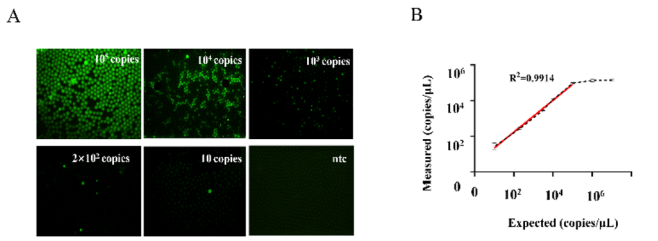

Fig. 4 Single-molecule IVA RNA detection and quantification. (A) Representative end-point fluorescence images of various IVA RNA concentrations for the digital droplet Cas13a assay (4× magnification). (B) Quantification range of the digital droplet Cas13a assay.

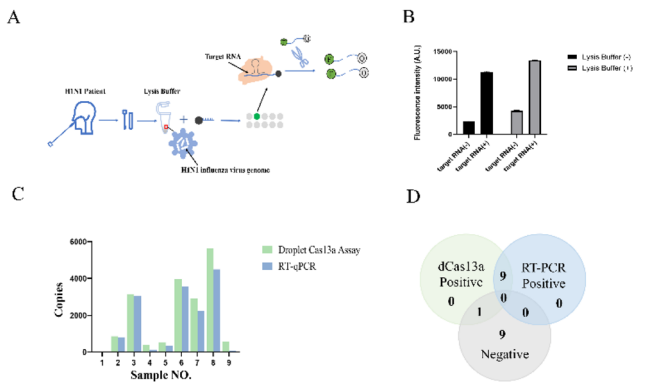

Fig. 5 Digital droplet Cas13a assay for the detection of clinical samples of IVA. (A) Schematic of the clinical diagnosis of IVA using the digital droplet Cas13a assay. The target RNA was extracted from clinical nasopharyngeal swab samples. (B) The effect of lysis buffer on the reaction. (C) Comparison of the RT-qPCR system and our afDDA method for detecting IVA (9 positive and 10 negative samples). (D) Detection results of RT-qPCR and afDDA methods for detecting the 9 positive samples.

Conclusions

To summarize, we achieved digital detection of influenza A viral RNA by combining droplet microfluidics with CRISPR/Cas13a technology. Target RNA-containing droplets can produce background-specific signals in less than half an hour under ideal experimental conditions without the need for reverse transcription or amplification. This led to faster reaction times and superior sensitivity and specificity. The issue that traditional digital assays cannot detect low quantity targets in big sample volumes can be resolved by using polystyrene microspheres to assist target extraction and enrichment from large sample volumes. In the future, we will attempt to encode polystyrene microspheres in order to develop a technique that employs Cas13a for the development of multiplexed RNA tests on a single chip. The results of this study show that the RNA detection technology based on droplet microfluidics and Cas13a is a powerful tool in the field of absolute molecular quantification and has a broad clinical application prospect.

Author contributions

Jiayan Liu: writing – original draft, methodology, investigation, and data curation. Taixue An, Jingjie Peng, and Qinjiang Zhu: writing – review & editing and methodology. Heyang Zhao and Zhiyu Liang: methodology and data curation. Kai Mo: project administration and funding acquisition. Tiancai Liu: project administration, methodology, and funding acquisition. Kun Wu: supervision and project administration.

Data availability

Data will be made available on request.

Conflicts of interest

There are no conflicts to declare.

This journal is © The Royal Society of Chemistry 2025

Published on 14 febbraio 2025. Downloaded on 14/02/2026 03:50:15.

Acknowledgements

The work was financially supported by grants from the National Natural Science Foundation of China (grant no. 82372344), the Natural Science Foundation of Guangdong Province (grant no. 2023A1515011925), and the Guangdong Basic and Applied Basic Research Foundation (no. 2021A1515220006 and 2022A1515010410) to KM.

References

1 L. Ferguson, A. K. Olivier, S. Genova, W. B. Epperson, D. R. Smith, L. Schneider, K. Barton, K. McCuan, R. J. Webby and X. F. Wan, *J. Virol.*, 2016, **90**, 5636–5642.
2 M. Worobey, G. Z. Han and A. Rambaut, *Proc. Natl. Acad. Sci. U. S. A.*, 2014, **111**, 8107–8112.
3 J. S. Long, B. Mistry, S. M. Haslam and W. S. Barclay, *Nat. Rev. Microbiol.*, 2019, **17**, 124–124.
4 K. Lewandowski, Y. Xu, S. T. Pullan, S. F. Lumley, D. Foster, N. Sanderson, A. Vaughan, M. Morgan, N. Bright, J. Kavanagh, R. Vipond, M. Carroll, A. C. Marriott, K. E. Gooch, M. Andersson, K. Jeffery, T. E. A. Peto, D. W. Crook, A. S. Walker and P. C. Matthews, *J. Clin. Microbiol.*, 2019, **58**(1), e00963–e00919.
5 S. Yamayoshi and Y. Kawaoka, *Nat. Med.*, 2019, **25**, 212–220.
6 M. Hussain, H. D. Galvin, T. Y. Haw, A. N. Nutsford and M. Husain, *Infect. Drug Resist.*, 2017, **10**, 121–134.
7 C. Farre, S. Viezzi, A. Wright, P. Robin, N. Lejal, M. Manzano, J. Vidic and C. Chaix, *Anal. Bioanal. Chem.*, 2022, **414**, 265–276.
8 J. Ellis, M. Iturriza, R. Allen, A. Bermingham, K. Brown, J. Gray and D. Brown, *Eurosurveillance*, 2009, **14**(22), 19230.
9 Y. Yao, X. Chen, X. Zhang, Q. Liu, J. Zhu, W. Zhao, S. Liu and G. Sui, *ACS Sens.*, 2020, **5**, 1354–1362.
10 H. Cui, C. Zhang, F. Tu, K. Zhao, Y. Kong, J. Pu, L. Zhang, Z. Chen, Y. Sun, Y. Wei, C. Liang, J. Liu, J. Liu and Z. Guo, *Front. Cell. Infect. Microbiol.*, 2022, **12**, 1071288.
11 H. Chen, S. G. Park, N. Choi, J. I. Moon, H. Dang, A. Das, S. Lee, D. G. Kim, L. Chen and J. Choo, *Biosens. Bioelectron.*, 2020, **167**, 112496.
12 B. J. Park, M. S. Park, J. M. Lee and Y. J. Song, *Biosensors*, 2021, **11**(3), 88.
13 G. Neumann, T. Noda and Y. Kawaoka, *Nature*, 2009, **459**, 931–939.
14 Z. Mumtaz, Z. Rashid, A. Ali, A. Arif, F. Ameen, M. S. AlTami and M. Z. Yousaf, *Biosensors*, 2023, **13**(6), 584.
15 J. Liu, B. Zhang, L. Wang, J. Peng, K. Wu and T. Liu, *Anal. Methods*, 2024, **16**, 971–978.
16 A. Basiri, A. Heidari, M. F. Nadi, M. T. P. Fallahy, S. S. Nezamabadi, M. Sedighi, A. Saghazadeh and N. Rezaei, *Rev. Med. Virol.*, 2021, **31**, 1–11.
17 K. M. Shen, N. M. Sabbavarapu, C. Y. Fu, J. T. Jan, J. R. Wang, S. C. Hung and G. B. Lee, *Lab Chip*, 2019, **19**, 1277–1286.
18 Z. Li, L. Y. Hua, L. M. Xie, D. Wang and X. Y. Jiang, *Anal. Chem.*, 2023, **95**, 6940–6947.
19 Y. T. Shang, G. W. Xing, J. X. Lin, Y. X. Li, Y. N. Lin, S. L. Chen and J. M. Lin, *Biosens. Bioelectron.*, 2024, **243**, 115771.
20 G. H. Cao, D. Q. Huo, X. L. Chen, X. F. Wang, S. Y. Zhou, S. X. Zhao, X. G. Luo and C. J. Hou, *Talanta*, 2022, **248**, 123594.
21 J. Q. Cui, F. X. Liu, H. Park, K. W. Chan, T. Leung, B. Z. Tang and S. H. Yao, *Biosens. Bioelectron.*, 2022, **202**, 114019.
22 J. Y. Dong, X. Y. Wu, Q. S. Hu, C. S. Sun, J. H. Li, P. Song, Y. Su and L. Zhou, *Biosens. Bioelectron.*, 2023, **241**, 115673.
23 R. Bruch, J. Baaske, C. Chatelle, M. Meirich, S. Madlener, W. Weber, C. Dincer and G. A. Urban, *Adv. Mater.*, 2019, **31**, e1905311.
24 P. W. Qin, M. Park, K. J. Alfson, M. Tamhankar, R. Carrion, J. L. Patterson, A. Griffiths, Q. He, A. Yildiz, R. Mathies and K. Du, *ACS Sens.*, 2019, **4**, 1048–1054.
25 T. Tian, B. W. Shu, Y. Z. Jiang, M. M. Ye, L. Liu, Z. H. Guo, Z. P. Han, Z. Wang and X. M. Zhou, *ACS Nano*, 2021, **15**, 1167–1178.
26 Y. X. Zhang, Y. Song, Z. Y. Weng, J. Yang, L. Avery, K. D. Dieckhaus, R. B. C. Lai, X. Gao and Y. Zhang, *Lab Chip*, 2023, **23**, 3862–3873.
27 X. Y. Shan, F. Gong, Y. X. Yang, J. J. Qian, Z. Y. Tan, S. B. Tian, Z. K. He and X. H. Ji, *Anal. Chem.*, 2023, **95**, 16489–16495.